# Morphological and raman effects on $^{252}$Cf irradiated diamond

C. Vázquez-López[a], G. Espinosa[b], J.I. Golzarri[b], and S. Jiménez-Sandoval[c]
[a] *Departamento de Física, Centro de Investigación y de Estudios Avanzados del I.P.N., apartado postal 14-740, México 07000, D.F. México.*
[b] *Instituto de Física, Universidad Nacional Autónoma de México, apartado postal 20-364, México, D.F.*
[c] *Centro de Investigación y de Estudios Avanzados del I.P.N. Unidad Querétaro, apartado postal 1-798, Querétaro, México.*
*e-mail: cvlopez@fis.cinvestav.mx.*

Recibido el 14 de mayo de 2007; aceptado el 26 de octubre de 2007

Radiation damage produced by the incidence of fission fragments from a californium ($^{252}$Cf) source into diamond is characterized by atomic force microscopy and Raman spectroscopy. In comparison with the original non irradiated surface, it was found cavities and hillock-like regions. By micro-Raman spectroscopy, it was revealed changes in the crystalline structure: there are graphite-like regions and nanostructured diamond regions.

*Keywords:* diamond; atomic force microscopy; Raman spectroscopy; nuclear tracks

El daño por irradiación de fragmentos de fisión procedentes de una fuente de californio ($^{252}$Cf) sobre diamante ha sido caracterizado por microscopía de fuerza atómica y por espectroscopía Raman. Comparando con la superficie no irradiada, se encontraron cavidades y protuberancias. Por espectroscopia Raman se determinaron cambios en la estructura cristalina: existen regiones grafíticas y regiones nanoestructuradas.

*Descriptores:* diamante; microscopía de fuerza atómica; trazas nucleares.

PACS: 29.25.Rm; 68.37.Ps; 78.30.-j; 81.05.Uw

## 1. Introduction

Atomic force microscopy (AFM) is an invaluable measuring technique to observe surface defects after low energy or swift heavy ion irradiation [1-3]. Raman spectroscopy has become a powerful tool in the analysis of carbon in all the different allotropic states, due to its ability to distinguish different bonding types, domain size and its sensitivity to internal stresses [4]. The Raman peak shift, the shape, half-width, intensity and polarisation are each parameters that provide information about chemistry and structure. The intensity of a Raman peak is directly proportional to the concentration of scattering species under analysis which provides a basis for quantitative analysis.

Natural diamond exhibits one main Raman active vibration which manifests itself as a sharp first order peak in the Raman spectrum at $\sim 1332$ cm$^{-1}$, with full-width at half the peak height (FWHM) typically $< 2$ cm$^{-1}$[5]. In this paper, the influence of irradiation of fission fragments from $^{252}$Cf on the surface morphology and of the Raman spectrum of diamond is reported.

## 2. Experimental

A crystalline diamond sample whose face on which the particles irradiation were incident, (the table) was (102) oriented, as determined by a single crystal diffractometer Enras-Nonius Kappa CCD. The sample was cleaned in a 3:1 $H_2SO_4$/$HNO_3$ acid at ca 90$^o$C followed by $H_2O$ rinsing and ultrasonic cleaning in acetone and ethanol [6].

The radiation source was an electrodeposited $^{252}$Cf, with a binary distribution of the predominant energies of 79.4 and 103.8 MeV, with a flux of 98 fission fragments (ff) per min/cm$^2$. Irradiations were made in air, with the source in contact with the target through an aluminum foil, 10 microns thick, and through which collimating holes (approximately 100-150 $\mu$m) had been made by pricks with a fine needle. Thus the ff$'$s were collimated approximately normal to the target surface.

The calculated rate of surface impacts was larger than 1 ff per week per area of 10,000 $\mu$m$^2$. Irradiations were made for up to 20 days and produced more than 5 impacts per zone of 10 $\mu$m x 10 $\mu$m as observed by AFM.

Raman scattering measurements were performed at ambient temperature in a Dilor Micro-Raman system, model Labram by focusing at 50:1. The signal was detected with a thermoelectrically cooled low-noise CCD detector. An $Ar^+$ ion laser was used as excitation source employing the 488 nm emission line.

## 3. Results and discussion

An AFM micrograph of the diamond surface, before irradiation, is shown in Fig. 1A, details of the polishing grooves are observed. In Fig. 1B, an AFM image of the sample irradiated during 20 days is shown. The scale shows that the irregularly shaped craters and the hillocks have dimensions of up to a few tenths microns.

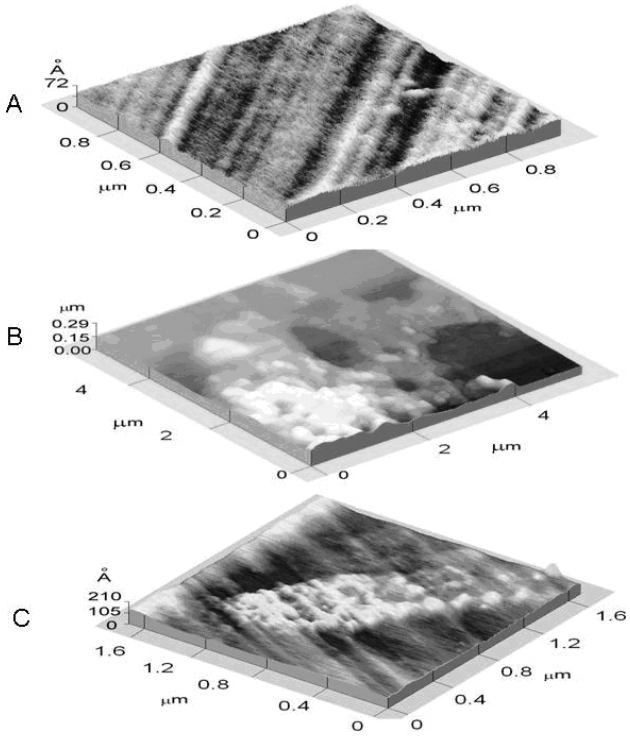


FIGURE 1. Diamond surface images. A) original surface; B) after exposure to fission fragments; and C) after exposure and cleaning.

Let us now consider the physical processes involved in ff impacts on the targets, and their relevance to the observations we have seen. The fundamental sputtering process is one of converting the forward momentum of the projectile into reverse momentum of the target components - the ion explosion-spike model [7]. The projectile ions, having energies of the order 100 MeV, produce a rich halo of ejecta ions that, after neutralization, condense back on the target surface. The main damaged region around the trajectory of each incident particle is estimated as a cylindrical core of radius less than thousands atomic distances [8].

There are also craters formations at impact zones. The irradiations were conducted under atmospheric conditions so that some oxidation of carbon ions would have taken place in the plasma haloes, as well as at the impacts sites themselves. Then ff's produce damage tracks penetrating into the bulk of the targets. The damage tracks below the surface are largely invisible to the AFM. The penetration range of the ff's in diamond was calculated using TRIM-2003.26. Most ff's penetrate to a depth of about 8 microns.

Hillocks of the size observed in Fig. 1B can not be produced by an individual impact. It is rather plausible that some atmospheric polluting effect could have induced such hillocks, around smaller features produced by the impacts. In order to verify such effect, we performed a cleaning process of the sample, following the procedure of Ref. 6. In Fig. 1C, an AFM image of the sample is presented, after the cleaning process. The topography of the sample has a roughness in accordance with the original polishing grooves, as well as a plausible sputtering effect due to the incident fission fragments.

The crystalline form of the condensed carbon ejecta and of the cratering regions might be another allotrope of carbon. In order to identify such structures, micro Raman scattering experiments was done. Figure 2A shows a Stokes Raman spectrum taken on a non irradiated region of the sample. The main peak at 1334 cm$^{-1}$ is the characteristic feature of natural cubic diamond. The peak amplified a factor five and centered at 1737 cm$^{-1}$ is a photoluminescence feature due to impurities in the crystal. This peak is absent in the Anti-Stokes spectrum.

Two kinds of induced effects were observed: regions in which the produced disorder is high, a graphite-like band is observed. The Raman spectrum in Fig. 2B shows this effect as an additional peak centered at 1560 cm$^{-1}$ (G peak). The G peak has been attributed to carbon atoms hybridizing with sp$^2$ bonds [9]. In addition, a variable background appears which corresponds to fluorescence by induced defects and/or local amorphisation of the material [5]. In spite of the minimal graphitic material that might be present in some cavities, it is worth to take into account that at 488 nm the laser penetration depth in graphite is 50 nm and that the scattering efficiency ratio relative to diamond has been reported to be 50 times larger for graphite [10]. Regions in which the disorder is mild, nanocrystalline diamond is generated. In the Raman spectrum of Fig. 2C, this kind of influence of the irradiation is shown.

The peak centered at 1138 cm$^{-1}$ corresponds to nanocrystalline diamond or disordered sp$^3$-bonded carbon which forms as a precursor to diamond formation [11]. The relative intensity of the 1334 cm$^{-1}$ peak with respect to that at 1138 cm$^{-1}$ indicates that the predominant material in the probed region corresponds to non-damaged diamond. In this spectrum there is no evidence of the formation of graphite.

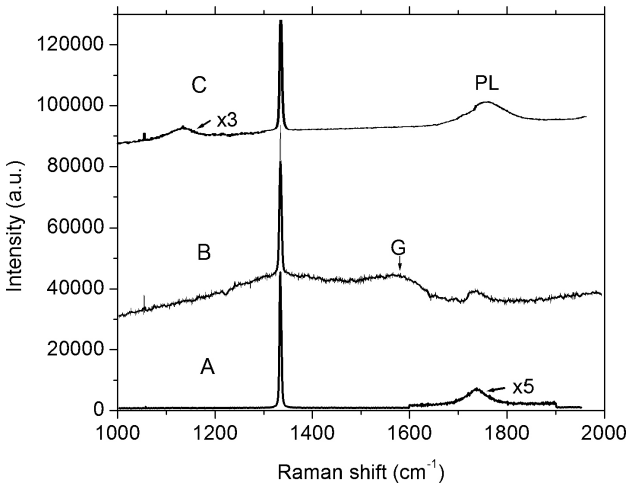


FIGURE 2. A) First order Raman spectra for matrix region; B) damaged region with graphite-like carbon and disorder; and C) damaged region with nanocrystalline diamond.

## 4. Conclusions

Three kinds of morphological surface effects produced by $^{252}$Cf fission fragments on diamond were observed: By AFM it was determined that hillocks and cavities were produced. By micro Raman spectroscopy structural changes were observed around the cavities and hillocks: graphite-like carbon, nanocrystalline diamond regions and structural disorder.

## Acknowledgements

The authors wish to thank to Rogelio Fragoso, Blanca Zendejas, Alejandra García, Marco Antonio Leyva, and F. Rodríguez M. for their technical assistance. This work was partially supported by PAPIIT-DGAPA-UNAM grant IN107707.

1. C.M. Demanet, S. Shrivastava, and S. Sellschop, *Surf. and Interface Analysis*, **23** (1995) 115.
2. M. Kappel, M. Steidl, J. Biener, and J. Kuppers, *Surf. Sci. Lett.* **387** (1997) L1062.
3. C. Vázquez-López *et al.*, *Radiat. Meas.* **34** (2001) 189.
4. R.E. Shroeder and R.J. Nemanich, *Phys. Rev. B* **41** (1990) 3738.
5. P.K. Bachmann and D.U. Wiechert, in *Diamond and Diamond-Like Films and Coatings*, edited by R.E. Clausing *et al.*, Plenum Press, (New York 1991).
6. R.J.A. van den Oetelaar and C.F.J. Flipse, *Surf. Sci. Lett.* **384** (1997) L828.
7. G. Espinosa. *Trazas Nucleares en Sólidos*, UNAM, (México, 1994)
8. V.A. Ditlov, *Radiat. Meas.* **31** (1999) 57.
9. A.M. Bonnot, *Phys. Rev. B* **41** (1990) 6040.
10. N. Wada, P.J. Gaczi, and S.A. Solin, *J. Non-Crystalline Solids* **35** (1980) 543.
11. R.J. Nemanich, J.T. Glass, G. Lucovsky, and R.E. Shroder, *J. Vac. Sci. Technol. A* **6** (1988) 1783.